Accepted Manuscript

Characterization and structure-activity relationship study of iminodipyridinopyrimidines as novel hepatitis C virus inhibitor

Dong-Sik Park, Eunji Jo, Jihyun Choi, MyungEun Lee, Soohyun Kim, Hee-Young Kim, Jiyon Nam, Sujin Ahn, Jong Yeon Hwang, Marc Peter Windisch

PII: S0223-5234(17)30692-X

DOI: 10.1016/j.ejmech.2017.09.010

Reference: EJMECH 9725

To appear in: *European Journal of Medicinal Chemistry*

Received Date: 3 April 2017

Revised Date: 23 August 2017

Accepted Date: 5 September 2017

Please cite this article as: D.-S. Park, E. Jo, J. Choi, M. Lee, S. Kim, H.-Y. Kim, J. Nam, S. Ahn, J.Y. Hwang, M.P. Windisch, Characterization and structure-activity relationship study of iminodipyridinopyrimidines as novel hepatitis C virus inhibitor, *European Journal of Medicinal Chemistry* (2017), doi: 10.1016/j.ejmech.2017.09.010.

Graphical Abstract

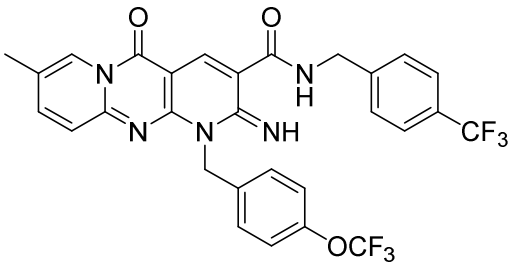

12c

HCVcc EC_{50} = 10 nM; HCVcc CC_{50} > 20 uM; Selectivity Index (SI) > 2000
HCVrp : inactive
HCVpp : minor activity
Liver microsomes ($t_{1/2}$) > 60 min in rat and human

Characterization and structure-activity relationship study of iminodipyridinopyrimidines as novel hepatitis C virus inhibitor

Dong-Sik Park[a,#], Eunji Jo[b,#], Jihyun Choi[a], MyungEun Lee[b], Soohyun Kim[b], Hee-Young Kim[b], Jiyon Nam[c], Sujin Ahn[c], and Jong Yeon Hwang[a,d,*], Marc Peter Windisch[b,*]

[a]Medicinal Chemistry Group, Institut Pasteur Korea, Seongnam-si, Gyeonggi-do, Republic of Korea;

[b]Applied Molecular Virology, Institut Pasteur Korea, Seongnam-si, Gyeonggi-do, Republic of Korea;

[c]DMPK Group, Institut Pasteur Korea, Seongnam-si, Gyeonggi-do, Republic of Korea;

[d]Bio&Drug Discovery Division, Korea Research Institute of Chemical Technology, PO Box 107, Daejeon 305-600, Republic of Korea

[#]These authors equally contributed to this work.

*Corresponding authors. Email: jyhwang@krict.re.kr and marc.windisch@ip-korea.org

Abstract

Upon high-throughput screening of synthetic small molecule libraries with the infectious hepatitis C virus (HCV) cell culture system, we identified an iminodipyridinopyrimidine (IDPP) scaffold. IDPP did not inhibit HCV replication, but exhibited very potent inhibitory activity on early and late steps of HCV life cycle. Applying an intensive structure-activity relationship (SAR) study, a promising IDPP Lead compound (**12c**) with excellent potency (EC_{50} = 10 nM), high safety margin (SI >2,000), and an acceptable stability in human and rat liver microsomes ($t_{1/2}$ >60 min) was identified. Overall, our results suggest that the IDPP scaffold could be used for the development of novel HCV interventions.

1. Introduction

About 3% of the global population is chronically infected with the hepatitis C virus (HCV) which is a major cause of chronic liver diseases potentially leading to hepatocellular carcinoma (HCC) [1]. For decades the standard-of-care (SOC) was a combination of pegylated interferon-alpha (PEG-IFNα) and ribavirin (RBV) associated with an unsatisfactory sustained virologic response rate (SVR) of only 70-80 % accompanied with partially severe side effects [2-5]. With the recent FDA approval of direct-acting antiviral agents (DAAs) such as sofosbuvir, daclatasvir, etc. powerful drugs to tackle chronic hepatitis C (CHC) are now available for therapy [6, 7]. However, all drugs exclusively interfere with viral replication whereas drugs targeting other steps of the HCV life cycle have not been developed yet. Utilizing the infectious HCV cell culture (HCVcc) system, which enabled to study the entire viral life cycle, led to the identification of small molecules, such as, green-tea polyphenolepigallocatechin-3-gallate (EGCG), HCV II-1, flunarizine, etc. shown to interfere with glycoprotein E1 and E2 mediated HCV entry[8-13]. Targeting entry tackles a viral infection at its initial step prior to the multiplication of the virus genomic material which may reduce the emergence of viral drug resistance. Furthermore, HCV entry inhibitors are predestinated of preventing reinfection of transplanted livers and of inhibiting the vertical transmission of the virus.

In this context, we set up the infectious HCV genotype 2 cell culture system and screened small molecule compound libraries to identify new antiviral agents with a novel mechanism of action (MoA) [14]. In order to enrich for hits with a novel MoA, we excluded hits active in the HCV replicon system, thereby removing replication inhibitors which are dominant drug candidates in clinical development. Furthermore, selected hits were evaluated and characterized in a series of secondary assays and to identify the putative molecular target. From this rational drug discovery approach, we identified an iminodipyridinopyrimidine (IDPP) scaffold very potently inhibiting the HCV life cycle, which encouraged us to explore further the potential of IDPPs as a novel anti-HCV agent by conducting a structure-activity relationship (SAR) study. Here we report the identification, synthesis and SAR study of IDPPs.

2. Results and discussion

2.1. High throughput screening campaign and hit selection.

More than 200,000 small molecules were screened at 6 μM concentration against the entire HCV life cycle. Hits were selected according >70% HCV inhibition and >70% cell viability criteria and confirmed by 10-point dose-response curve (DRC) analysis in the high throughput screening (HTS) assay. Thereby, the half maximal effective concentration against entirety inhibit the entire HCV life cycle (EC_{50}), as well as the cytotoxic concentration (CC_{50}), was determined to calculate selectivity index (SI) values (CC_{50}/EC_{50}). Confirmed active hits with an SI >10 were triaged in HCV pseudoparticle (HCVpp) and replicon (HCVrp) systems to determine inhibitory effects on viral entry and viral RNA replication, respectively. Following this approach, we identified a series of IDPPs with potent anti-HCV activity in the infectious cell culture system (Figure 1). The representative IDPP **1** exhibited strong inhibitory activity against HCVcc without any cytotoxicity (Figure 2A). The preliminary SAR analysis with IDPP analogs, screened with DRC analysis in the primary HTS assay, revealed that hydrophilic or short alkyl substitution such as ethyl, propyl, isopropyl, morpholine, or methoxyethyl on either R^2 or R^3 of IDPPs showed very weak or no inhibitory HCV activity (data not shown). IDPP **1** was shown to be inactive in the HCV replicon system (EC_{50} >30 μM) (Figure 2B). Interestingly, IDPP inhibited specifically E1/E2-mediated viral entry as shown by experiments with HCVpp, whereas vesicular stomatitis virus pseudoparticle (VSVpp) were not inhibited (Figure 2C). Furthermore, utilizing a virus supernatant transfer assay, it was demonstrated that IDPP interfered with the secretion of infectious HCV particle (data not shown). Taken together, these results demonstrate that IDPP has a novel MoA by interfering with the early and late steps of the HCV life cycle which encouraged us to conduct an in-depth SAR study with the goal to move from hit towards Lead.

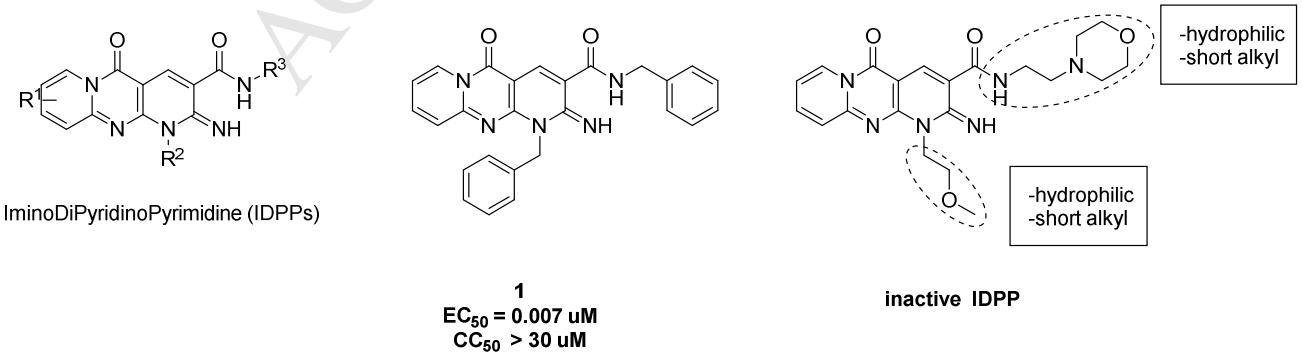

Figure 1. The representative structure of IDPP (left), active hit IDPP **1** (middle), and inactive IDPP (right).

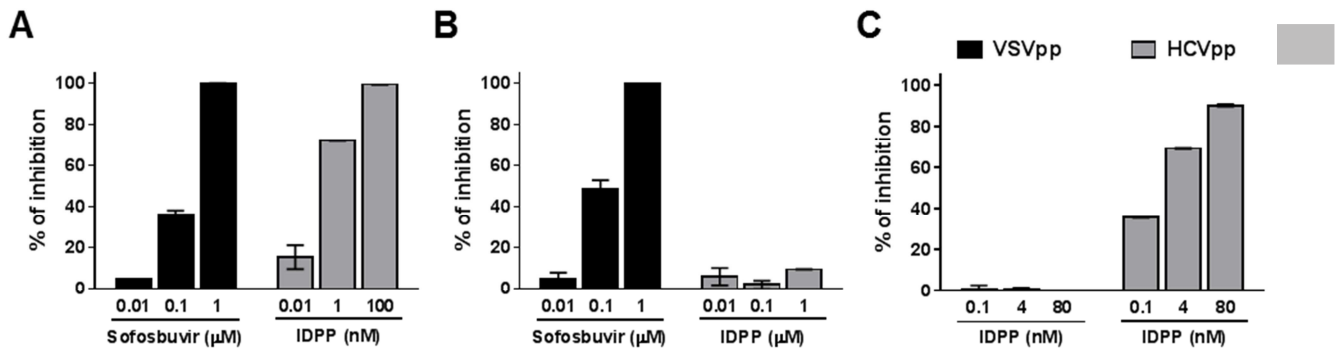

Figure 2. Biological activity of IDPP. (A) Evaluation of IDPP 1 in the HCVcc system. Huh-7.5 cells were seeded in 384-well plate and exposed to compounds at indicated concentrations (0.01, 0.1 and 1 μM) for 2 h followed by infection of HCVcc. Sofosbuvir, an HCV RNA polymerase inhibitor, was used as a positive control. Anti-HCV activity was determined at day 3 post infection as described in material and methods. (B) Evaluation of IDPP 1 in the HCVrp system. Replicon cells were seeded in 384-well plate and treated with compounds and analyzed as described above. (C) Evaluation of IDPP 1 in the HCVpp system. Huh-7.5 cells were seeded in 384-well plate and treated with compounds for 2 h followed by transduction with VSVpp or HCVpp.

2.2. Chemistry.

The representative synthesis of IDPPs was depicted in Scheme 1. The key intermediate chloro-aldehyde **4** were prepared as described elsewhere [15]. Briefly, 2-hydroxypyridopyrimidinones **3** were prepared by cyclization of 2-aminopyridines **2** and highly reactive bis (2,4,6-trichlorophenyl) malonate. Then **3** were treated with $POCl_3$ and DMF to afford chloro-aldehyde **4**. Treatment of amines for R^2 and subsequent 1 N aqueous HCl hydrolysis gave aldehyde **5**. Aldehydes **5** were subjected to Knoevenagel condensation with ethylcyanoacetate to afford ester IDPPs **6** [16] that were hydrolyzed to carboxylic acids **7** by the treatment of LiOH. Carboxylic acids **7** were converted to the desired IDPPs **8** by treatment with various amines using BOP as a coupling agent. IDPPs **9** bearing cyano, carboxamide, and sulfonyl were prepared from intermediate **5a** by treatment of the corresponding nitriles such as malononitrile, cyanoacetamide, sulfonylacetonitrile, respectively.

Scheme 1. General synthetic method for IDPP analogs.

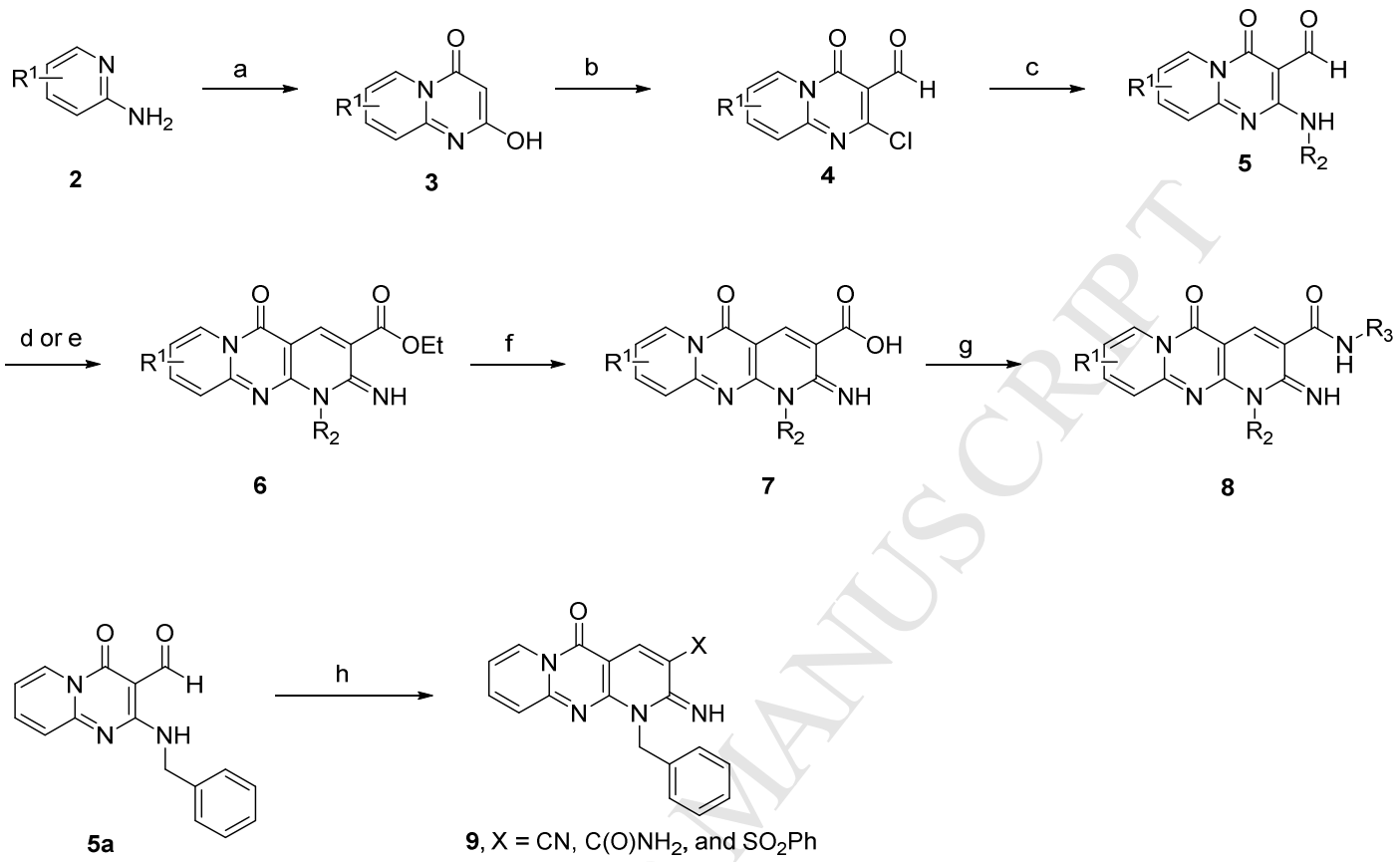

Scheme 1. Reagents and conditions: (a) bis(2,4,6-trichlorophenyl) malonate, acetone, rt, 18 h; (b) $POCl_3$, DMF, 0°C to rt, 2 h; (c) i) R_2NH_2, TEA, 70°C, 18 h; ii) 1 *N* aq. HCl/THF (1:3), 70°C, 1 h; (d) i) 2-methoxyethylamine, MeOH, 50 °C, 18 h; ii) ethylcyanoacetate, $CHCl_3$, 70°C, 18 h; (e) ethylcyanoacetate, piperidine, molecular sieve, EtOH, rt, 1-2 days; (f) LiOH, H_2O, THF, rt, 24 h; (g) R_3NH_2, BOP, NMM, DMF, rt, 18 h; (h) nitriles, piperidine, EtOH, rt.

2.3. Structure-activity relationship study

Upon identification of IDPP **1** as an active hit, we set out to understand the key structural elements that were responsible for anti-HCV inhibitory potency. First, the tolerability of amide in IDPPs by replacement with several functional groups including ester, acid, nitrile, carboxamide, and sulfone was examined (Table 1). IDPP **1** showed very potent anti-HCV activity with low cytotoxicity (EC_{50}= 0.007 μM and CC_{50}> 30 μM),

thus providing an excellent SI value (SI >4,285). The nitrile **9a**, carboxamide **9b**, and sulfone **9c** showed at least 14-fold reduced potencies (EC_{50}= 0.35, 0.16, 0.1 μM, respectively) compared to **1**. Only ester **6a** displayed a slightly reduced activity and increased cytotoxicity (EC_{50}= 0.015 μM and CC_{50}= 17 μM) thus showing lower SI value (SI= 1,121) compared to **1** (SI >4,286). Carboxylic acids **7a** displayed poor anti-HCV activity (EC_{50}= 6.0 μM).

Table 1. Anti-HCV activity of IDPP **1**, **6a**, **7a**, and **9a-9c**.

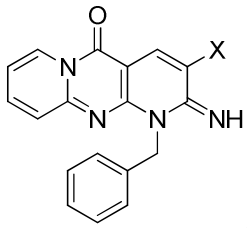

No.	X	EC_{50} (μM)	CC_{50}(μM)	SI (CC_{50}/EC_{50})
1	-CONHBn	0.007	> 30	> 4,286
6a	$-CO_2Et$	0.015 ± 0.001	17.0 ± 2.12	1,121
7a	$-CO_2H$	6.0	17.2	2.8
9a	-CN	0.35 ± 0.01	> 20	> 57
9b	$-CONH_2$	0.16	> 20	> 125
9c	$-SO_2Ph$	0.10 ± 0.03	> 20	> 200

EC_{50} and CC_{50} values were determined by 10-point DRC analysis in duplicates with quadruplicate measurements.

Table 2. Anti-HCV activity of IDPP **10a-10p**.

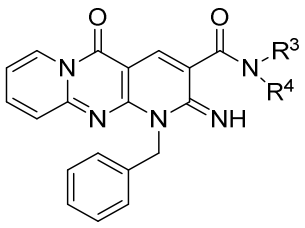

No.	R^3R^4NH	EC_{50} (μM)	CC_{50}(μM)	SI (CC_{50}/EC_{50})	Metabolic stability Human / Rat ($t_{1/2}$, min)
1	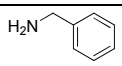	0.007	> 30	> 4,286	55/9

8a	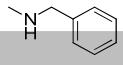	0.030 ± 0.001	> 6.7	> 222	1.8/1.5
8b	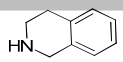	0.140 ± 0.01	8.2 ± 1.9	61	2.8/1.4
8c	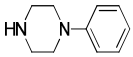	0.048 ± 0.007	10.1 ± 5.8	209	8.6/3.6
8d	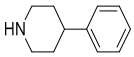	0.105 ± 0.05	> 10	> 95	58/5.6
8e		2.053 ± 0.21	> 20	> 9.8	127.7/24
8f		0.040 ± 0.008	> 20	> 445	n.d.
8g	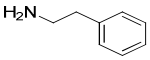	0.001 ± 0.0003	7.00 ± 0.95	7,000	3.0/1.5
8h	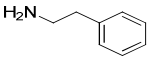	0.001 ± 0.0003	8.5 ± 0.95	8,847	4.3/2.0
8i	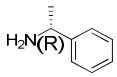	0.034 ± 0.0009	15.6 ± 1.26	459	40/18
8j	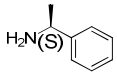	0.004 ± 0.0004	26.6 ± 6.27	6,650	15/6
8k	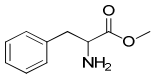	0.190 ± 0.06	8.4 ± 0.33	45	1.4/1.3
8l	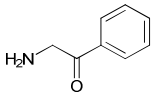	0.020 ± 0.0003	17.1	854	> 60/12.5
8m	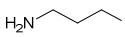	0.005 ± 0.004	> 20	> 4,000	34.4/7.5
8n	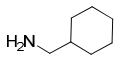	0.004 ± 0.0008	> 6.67	> 1,668	4.7/1.9
8o		0.003 ± 0.001	> 6.67	> 2,223	2.8/2.4
8p		0.003 ± 0.002	> 6.67	> 2,223	5.3/4.9

EC_{50} and CC_{50} values were determined by 10-point DRC analysis in duplicates with quadruplicate measurements. Not determined (n.d.).

Second, the effect of R^3R^4 substituents in IDPP was examined and the data was summarized in Table 2. Secondary amides such as *N*-methyl **8a**, isoquinoline **8b**, phenylpiperazine **8c**, phenylpiperidine **8d**, and morpholine **8e** generally reduced the anti-HCV activity (EC_{50}= 0.030-2.1 μM ranges). Particularly, hydrophilic morpholine substituted IDPP **8e** exhibited a drastically reduced potency. The phenyl **8f** displayed weaker inhibitory activity (EC_{50}= 0.040 μM) than benzyl **1**. Elongation of benzyl to phenethyl **8g** and phenylpropyl **8h** increased the potency (EC_{50}= 0.001 μM), however these modifications also increased cytotoxicity. Methyl substitution at immediately adjacent to nitrogen atom such as compound **8i** and **8j** showed good inhibitory activity (EC_{50}= 0.034 and 0.004 μM, respectively). Interestingly, S-isoform (**8j**) with methyl was approx. 9-fold more potent than the R-isoform (**8i**). Compounds **8k** and **8l** containing

hydrophilic carbonyl group decreased anti-HCV activity (EC_{50}= 0.19 and 0.020 μM, respectively) in comparison with **8 g** and **8h**. Hydrophobic aliphatic amines including n-butyl **8m**, cylcohexylmethyl **8n**, adamantyl **8o**, cyclohexyl **8p** showed very good inhibitory activity (EC_{50}= 0.004-0.005 μM ranges). In addition, the metabolic stability of IDPPs was evaluated in human and rat liver microsomal to predict *in vivo* pharmacokinetics. Compounds were incubated with liver microsomes and the half-life time ($t_{1/2}$, min) was determined. Surprisingly, the majority of compounds displayed poor microsomal stability against either human or rat (Table 2).

Table 3. Anti-HCV activity of IDPP **10a-10c**.

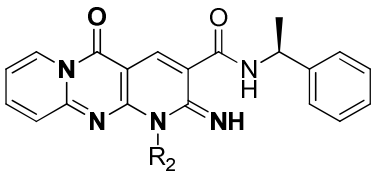

No.	R_2	EC_{50} (μM)	CC_{50}(μM)	SI (CC_{50}/EC_{50})
8j	Bn	0.004 ± 0.0004	26.6 ± 6.27	6,650
10a	H	Inactive	> 30	-
10b	Ph	0.42 ± 0.25	> 20	> 47.6
10c	CH_2-cHexcyl	0.004 ± 0.001	18.5	4,593

EC_{50} and CC_{50} values were determined by 10-point DRC analysis in duplicates with quadruplicate measurements.

Third, the effect of R^2 in IDPP was investigated (Table 3). In the primary HTS data analysis hydrophilic substituents containing oxygen or nitrogen in the R^2 group and short aliphatic side chain such as Me, Et, etc. were inactive. Given our early screening data, three compounds having H (**10a**), Ph (**10b**), and cyclohexylmethyl (**10c**) were evaluated for their anti-HCV activity. IDPP **10a** (R^2= H) was inactive and **10b** (R^2= Ph) had a significant lower anti-HCV activity (EC_{50}= 0.42 μM). The cyclohexyl methyl compound (**10c**) only showed equivalent potency (EC_{50}= 0.004 μM) with **8j**.

Table 4. Anti-HCV activity of IDPP **11a-11j**.

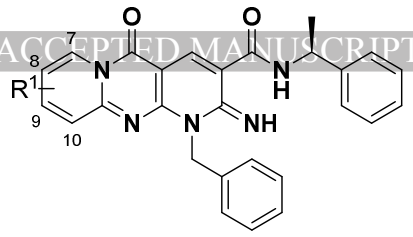

No.	R^1	EC_{50} (μM)	CC_{50}(μM)	SI (CC_{50}/EC_{50})	Metabolic stability Human / Rat ($t_{1/2}$, min)
8j	H	0.004 ± 0.0004	26.6 ± 6.27	6650	15 / 6
11a	8-Me	0.00009	> 20	> 221,385	10.7 / 3.6
11b	9-Me	0.00013	8.69	> 68,172	9.5 / 4.9
11c	10-Me	0.004 ± 0.001	5.60 ± 0.6	1,581	7.0 / 4.3
11d	10-MeO	0.002 ± 0.0008	7.47 ± 0.74	3,628	8.47 / 4.4
11e	8-F	0.002 ± 0.001	> 20	> 20,000	n.d.
11f	10-F	0.014 ± 0.015	> 20	> 20,000	n.d.
11g	8,10-F_2	0.003 ± 0.002	> 20	> 7,576	n.d.
11h	8-Cl	0.001 ± 0.001	> 20	> 13,841	n.d.
11i	10-Cl	0.06 ± 0.023	> 20	> 20,000	n.d.
11j	9-CF_3	0.007± 0.0004	> 20	> 2,719	n.d.

EC_{50} and CC_{50} values were determined by 10-point DRC analysis in duplicates with quadruplicate measurements. Not determined (n.d.).

We next studied the substituent effect on R^1 group of IDPPs and summarized the data in Table 4. Interestingly, all of the compounds investigated in the series showed strong inhibitory activity irrespectively with substituent R^1. Particularly, 8-Me (**11a**) and 9-Me (**11b**) substituted IDPP exhibited excellent anti-HCV activity with picomolar range (EC_{50}= 90 pM and 130 pM, respectively). In addition, **11a** displayed no cytotoxicity in the maximum concentration of the assay, resulting in an outstanding SI value (SI >221,385). However, all compounds substituents on the R^1 group had low human and rat microsomal stability. To overcome this issue, metabolite analysis of IDPP **1** in rat microsomal was performed, and the result suggested that major metabolites were hydroxylated or debenzylated IDPP as shown in Figure 3.

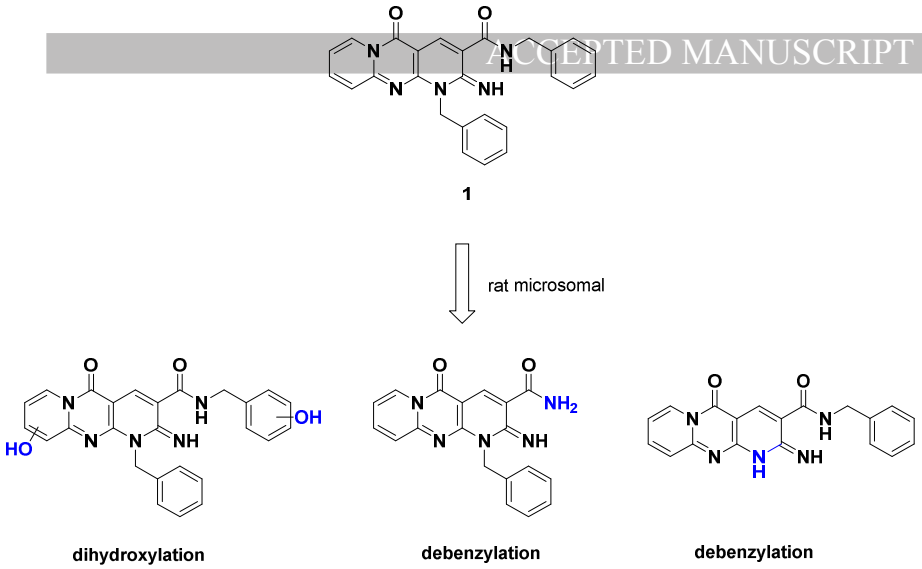

Figure 3. Detected metabolites induced by rat microsomes.

On the basis of the evaluation of IDPP analogs toward anti-HCV activity, cytotoxicity, and microsomal stability, we synthesized additional IDPP analogs to improve the balance between activity and stability. Among the additional compounds, four IDPP derivatives (12a-d) showing good microsomal stabilities in both human and rat were summarized in Table 5. As observed earlier in Table 4, compounds substituted with an 8-methyl at R^1 displayed very good anti-HCV activity without cytotoxicity. In addition, blocking of the potential metabolic labile site with substituents such as methyl, halogen, trifluoromethoxy, and phenyl in R^2 or R^3 successfully increased microsomal stabilities, thereby providing a promising Lead compound.

Table 5. Anti-HCV activity of IDPP **12a-12d**.

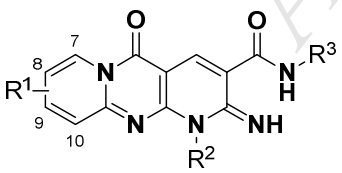

No.	**R¹**	**R²**	**R³**	EC_{50} (μM)	CC_{50} (μM)	SI (CC_{50}/	Metabolic stability Human /

					EC_{50})	Rat ($t_{1/2}$, min)
12a	8-Me	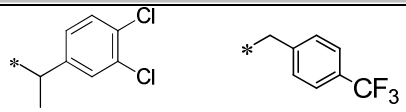	0.017 ± 0.0001	> 20	> 1,176	> 60 / > 60
12b	8-Me	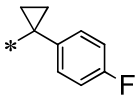	0.030 ± 0.48	> 20	> 2,041	> 60 / > 60
12c	8-Me	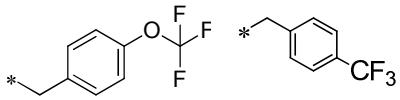	0.010 ± 0.0003	> 20	> 2,000	> 60 / > 60
12d	8-Me	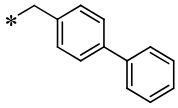	0.050 ± 0.008	> 20	> 2,198	> 60 / > 60

EC_{50} and CC_{50} values were determined by 10-point DRC analysis in duplicates with quadruplicate measurements.

3. Conclusion

In conclusion, a series of iminodipyridinopyrimidines (IDPPs) was identified by a phenotypic HTS assay using the infectious HCV cell culture system. IDPP **1** showed very potent anti-HCV activity with a favorable SI value. In addition, IDPPs were shown to be inactive in the HCV replicon system, indicating it has a distinct MoA from current DAAs which was reported by Lee *et al.* [17]. These results encouraged us to perform an SAR study to optimize IDPPs pharmacological properties. Through our intensive SAR study, we generated a promising IDPP Lead compound (**12c**) that showed excellent potency (EC_{50}= 10 nM), a good safety margin (SI >2,000), and an acceptable stability in human and rat liver microsomes ($t_{1/2}$ >60 min).

4. Experimental section

4.1. Chemistry

All materials were obtained from commercial suppliers and used without further purification. Solvents in this study were dried using an aluminum oxide column. Thin-layer chromatography was performed on pre-

coated silica gel 60 F254 plates. Purification of intermediates was carried out by normal phase column chromatography (MPLC, Silica gel 230-400 mesh). NMR spectra were recorded on a Varian 400 MHz. LC/MS data were obtained using a Waters 2695 LC and Micromass ZQ spectrometer. Identity of final compounds was confirmed by proton NMR and mass spectrometry.

4.1.1. The representative procedure for the preparation of compound 5. To a stirred solution of 2-chloro-4-oxo-4H-pyrido[1,2-a]pyrimidine-3-carbaldehyde (100 mg, 0.479 mmol) in THF (3 mL) was added benzylamine (0.058 mL, 0.527 mmol) and TEA (0.1 mL, 0.719 mmol). The reaction mixture was stirred at 70°C for 3 h. After the mixture was concentrated, 1 N aqueous HCl solution in THF (1/3 ratio, 4 mL). The reaction mixture was stirred at 70°C for 1 h. After reaction was completed, the mixture was evaporated and neutralized to approximately pH 7 by adding 1 *N* NaOH. The pale solid was collected by filtration and washed with H_2O to give **5a** (117 mg, 87%) as a brown solid. ^{1}H NMR (400 MHz, DMSO) δ 10.11 (s, 1H), 9.87 (t, *J* = 5.6 Hz, 1H), 8.81 (d, *J* = 8.0 Hz, 1H), 7.98 – 7.94 (m, 1H), 7.39 – 7.32 (m, 5H), 7.29 – 7.25 (m, 1H), 7.18 – 7.14 (m, 1H), 4.80 (d, *J* = 6.0 Hz, 2H)

4.1.2. The representative procedure for the preparation of compound 6. To a stirred solution of **5a** (86 mg, 0.310 mmol) in MeOH (1 mL) was added 2-methoxyethanamine (0.030 mL, 0.341 mmol). The mixture was stirred at 50°C overnight. After reaction was completed, the mixture was evaporated. To the residue in chloroform (2 mL) was added ethyl cyanoacetate (0.036 mL, 0.340 mmol) and stirred at 70°C overnight. After reaction was completed, the reaction mixture was diluted with EtOAc (20 mL) and washed with water (40 mL). The organic layer was dried over anhydrous $MgSO_4$ and concentrated *in vacuo*. The crude product was purified by flash column chromatography to give **6a** (97 mg, 84%) as a yellow solid. ^{1}H NMR (400 MHz, DMSO-d_6) δ 9.27 (s, 1H), 8.90 (d, J = 6.4 Hz, 1H), 8.47 (s, 1H), 8.05 – 8.00 (m, 1H), 7.58 (d, J = 8.8 Hz, 1H), 7.38 (d, J = 7.4 Hz, 1H), 7.34 – 7.29 (m, 2H), 7.26 (t, J = 7.4 Hz, 2H), 7.20 – 7.17 (m, 1H), 5.67 (s, 2H), 4.29 (q, J = 14.4, 7.2 Hz, 2H), 1.33 (t, J = 7.2 Hz, 3H); LCMS (electrospray) m/z $(M+H)^+$ 375

4.1.3. The representative procedure for the preparation of compound 7. To a stirred solution of **6a** (97 mg, 0.259 mmol) in THF (1 mL), MeOH (0.3 mL), and H_2O (0.6 mL) was added lithium hydroxide (62 mg, 2.6 mmol). The mixture was stirred at room temperature overnight. After reaction was completed, the mixture was evaporated and 1 *N* HCl (10.0 mL) was added to the residue to neutralize (pH 6). The pale solid

was collected by filtration and washed with H_2O to give **7a** (63 mg, 70%) as a brown solid. ^{1}H NMR (400 MHz, DMSO-d_6) δ 9.30 (brs, 1H), 9.04 (d, J = 6.4 Hz, 1H), 8.99 (s, 1H), 8.14 – 8.10 (m, 1H), 7.71 (d, J = 8.8 Hz, 1H), 7.45 (t, J = 6.8 Hz, 1H), 7.40 – 7.27 (m, 6H), 5.86 (s, 2H)); LCMS (electrospray) m/z $(M+H)^+$ 347.

4.1.4. The representative procedure for the preparation of compound 1, 8, 10, 11, and 12. To a stirred solution of **7a** (29 mg, 0.56 mmol) in DMF (1 mL) was added *N*-methylmorpholine (0.014 mL, 0.126 mmol), benzylamine (0.011 mL, 0.101 mmol) and benzotriazole-1-yl-oxy-tris-(dimethylamino)-phosphonium hexafluorophosphate (45 mg, 0.101 mmol). The reaction mixture was stirred at room temperature overnight. After reaction was completed, the reaction mixture was diluted with EtOAc (10 mL) and washed with saturated brine (20 mL). The organic layer was dried over anhydrous $MgSO_4$ and concentrated *in vacuo*. The crude product was purified by flash column chromatography to give **1** (7.0 mg, 20%) as a yellow solid. ^{1}H NMR (400 MHz, DMSO-d_6) δ 11.53 (t, *J* = 4.8 Hz, 1H), 9.25 (m, 1H), 9.16 (s, 1H), 8.97 (d, *J* = 7.2 Hz, 1H), 8.90 (d, *J* = 6.4 Hz, 1H), 8.10 (s, 1H), 8.03 – 7.96 (m, 2H), 7.77 (s, 1H), 7.61 – 7.55 (m, 1H), 7.39 – 7.17 (m, 7H), 5.65 (s, 2H), 4.46 (m, 2H); LCMS (electrospray) m/z $(M+H)^+$ 436

N,1-dibenzyl-2-imino-N-methyl-5-oxo-2,5-dihydro-1H-dipyrido[1,2-a:2',3'-d]pyrimidine-3-carboxamide (8a). Yellow solid; ^{1}H NMR (400 MHz, DMSO-d_6) δ 8.88 (d, *J* = 6.0 Hz, 1H), 7.97 (t, *J* = 8.0 Hz, 1H), 7.58 (s, 1H), 7.56 (s, 1H), 7.37 – 7.20 (m, 12H), 5.68 (s, 2H), 4.59 (brs, 2H), 2.87 (s, 3H); LCMS (electrospray) m/z $(M+H)^+$ 450

1-benzyl-2-imino-3-(1,2,3,4-tetrahydroisoquinoline-2-carbonyl)-1H-dipyrido[1,2-a:2',3'-d]pyrimidin-5(2H)-one (8b). Yellow solid; ^{1}H NMR (400 MHz, $CDCl_3$) δ 8.98 (d, *J* = 7.0 Hz, 1H), 7.92 (s, 1H), 7.78 (t, *J* = 8.8 Hz, 1H), 7.55 (d, *J* = 8.5 Hz, 1H), 7.44 (d, *J* = 7.4 Hz, 2H), 7.31 (t, *J* = 6.8 Hz, 3H), 7.21 - 7.11 (m, 6H), 5.84 (s, 2H), 4.78 (brs, 2H), 3.86 – 3.77 (m, 2H), 2.95 (s, 2H); LCMS (electrospray) m/z $(M+H)^+$ 462

1-benzyl-2-imino-3-(4-phenylpiperazine-1-carbonyl)-1H-dipyrido[1,2-a:2',3'-d]pyrimidin-5(2H)-one (8c). Yellow solid; ^{1}H NMR (400 MHz, DMSO-d_6) δ 8.90 (d, J = 7.0 Hz, 1H), 7.97 (t, *J* = 8.4 Hz, 1H), 7.61 – 7.57 (m, 2H), 7.39 (d, *J* = 7.5 Hz, 2H), 7.32 – 7.20 (m, 7H), 6.95 (d, *J* = 8.4 Hz, 2H), 6.81 (t, *J* = 7.2 Hz, 1H), 5.68 (s, 2H), 3.64 (brs, 4H), 3.14 (brs, 4H); LCMS (electrospray) m/z $(M+H)^+$ 491

1-benzyl-2-imino-3-(4-phenylpiperidine-1-carbonyl)-1H-dipyrido[1,2-a:2',3'-d]pyrimidin-5(2H)-one (8d). Yellow solid; ^{1}H NMR (400 MHz, $CDCl_3$) δ 8.95 (d, *J* = 6.4 Hz, 1H), 7.76 (s, 1H), 7.63 (ddd, *J* = 8.8, 6.8, 1.6 Hz, 1H), 7.51 - 7.45 (m, 3H), 7.34 – 7.27 (m, 4H), 7.25 – 7.18 (m, 5H), 7.07 (t, *J* = 7.2 Hz, 1H), 5.79 (s, 2H), 3.21 – 2.91 (brs, 2H), 2.81 – 2.75 (m, 1H), 1.99 – 1.87 (brs, 2H), 1.78 – 1.65 (m, 4H); LCMS (electrospray) m/z $(M+H)^+$ 490

1-benzyl-2-imino-3-(morpholine-4-carbonyl)-1H-dipyrido[1,2-a:2',3'-d]pyrimidin-5(2H)-one (8e). Yellow solid; ^{1}H NMR (400 MHz, DMSO-d_6) δ 8.90 (d, *J* = 7.6 Hz, 1H), 7.99 – 7.95 (m, 1H), 7.58 (d, *J* = 8.8 Hz, 1H), 7.55 (s, 1H), 7.46 (brs, 1H), 7.39 – 7.37 (m, 2H), 7.31 – 7.25 (m, 3H), 7.20 (d, *J* = 7.6 Hz, 1H), 5.66 (s, 2H), 3.63 – 3.56 (m, 4H), 3.55 -3.42 (m, 4H); LCMS (electrospray) m/z $(M+H)^+$ 416

1-benzyl-2-imino-5-oxo-N-phenyl-2,5-dihydro-1H-dipyrido[1,2-a:2',3'-d]pyrimidine-3-carboxamide (8f). Yellow solid; ^{1}H NMR (400 MHz, $CDCl_3$) δ 9.20 (s, 1H), 9.04 (d, *J* = 6.8 Hz, 1H), 7.79 – 7.75 (m, 1H), 7.70 (d, *J* = 8.4 Hz, 2H), 7.55 – 7.48 (m, 2H), 7.39 – 7.27 (m, 8H), 7.16 – 7.12 (m, 1H), 7.06 (dd, *J* = 14.0, 7.2 Hz, 1H), 5.70 (s, 2H); LCMS (electrospray) m/z $(M+H)^+$ 422

1-benzyl-2-imino-5-oxo-N-phenethyl-2,5-dihydro-1H-dipyrido[1,2-a:2',3'-d]pyrimidine-3-carboxamide (8g). Yellow solid; ^{1}H NMR (400 MHz, DMSO-d_6) δ 9.66 (brs, 1H), 8.97 (d, *J* = 6.8 Hz, 1H), 8.48 (brs, 1H), 8.05 (t, *J* = 7.6 Hz, 1H), 7.62 (d, *J* = 8.8 Hz, 1H), 7.39 – 7.20 (m, 12H), 5.74 (s, 2H), 3.48 (q, *J* = 14.0, 7.2 Hz, 2H), 2.84 (t, *J* = 6.8 Hz, 2H); LCMS (electrospray) m/z $(M+H)^+$ 450

1-benzyl-2-imino-5-oxo-N-(3-phenylpropyl)-2,5-dihydro-1H-dipyrido[1,2-a:2',3'-d]pyrimidine-3-carboxamide (8h). Yellow solid; ^{1}H NMR (400 MHz, $CDCl_3$) δ 9.05 (d, J = 7.2 Hz, 1H), 8.95 (s, 1H), 7.84 (t, *J* = 8.0 H, 1H), 7.54 (d, J = 8.8, 1H), 7.39 – 7.30 (m, 4H), 7.27 - 7.24 (m, 4H), 7.20 - 7.12 (m, 5H), 5.75 (s, 2H), 3.44 (dd, *J* = 12.8, 6.7 Hz, 2H), 2.70 (t, *J* = 7.6 Hz, 2H), 1.94 (dt, J = 14.5, 7.3 Hz, 2H) ; LCMS (electrospray) m/z $(M+H)^+$ 464

(R)-1-benzyl-2-imino-5-oxo-N-(1-phenylethyl)-2,5-dihydro-1H-dipyrido[1,2-a:2',3'-d]pyrimidine-3-carboxamide (8i). Yellow solid; ^{1}H NMR (400 MHz, DMSO-d_6) δ 11.66 (s, 1H), 9.23 (brs, 2H), 8.96 (d, *J* = 6.9 Hz, 1H), 8.73 (brs, 1H), 8.37 (brs, 1H), 8.02 (t, *J* = 8.0 Hz, 1H), 7.72 (brs, 1H), 7.60 (d, *J* = 8.8 Hz, 1H), 7.36 - 7.23 (m, 8H), 5.70 (s, 2H), 5.15 – 5.06 (m, 1H), 1.45 (s, 3H); LCMS (electrospray) m/z $(M+H)^+$ 450

(S)-1-benzyl-2-imino-5-oxo-N-(1-phenylethyl)-2,5-dihydro-1H-dipyrido[1,2-a:2',3'-d]pyrimidine-3-carboxamide (8j). Yellow solid; ^{1}H NMR (400 MHz, DMSO-d_6) δ 11.67 (s, 1H), 9.20 (brs, 2H), 8.95 (d, *J* = 6.9 Hz, 1H), 8.72 (brs, 1H), 8.30 (brs, 1H), 8.02 (t, *J* = 7.2 Hz, 1H), 7.72 (brs, 1H), 7.60 (d, *J* = 8.8 Hz, 1H), 7.36 - 7.23 (m, 8H), 5.69 (s, 2H), 5.13 – 5.07 (m, 1H), 1.45 (s, 3H); LCMS (electrospray) m/z $(M+H)^+$ 450

methyl 2-(1-benzyl-2-imino-5-oxo-2,5-dihydro-1H-dipyrido[1,2-a:2',3'-d]pyrimidine-3-carboxamido)-3-phenylpropanoate (8k). Yellow solid; ^{1}H NMR (400 MHz, $CDCl_3$) δ 9.02 (d, *J* = 7.2 Hz, 1H), 8.97 (brs, 1H), 7.76 (t, *J* = 7.6 Hz, 1H), 7.48 (d, *J* = 8.9 Hz, 1H), 7.37 – 7.29 (m, 4H), 7.24 - 7.12 (m, 9H), 5.62 (s, 2H), 5.00 (q, *J* = 13.2, 6.8 Hz, 1H), 3.67 (s, 3H), 3.21 – 3.11 (m, 2H); LCMS (electrospray) m/z $(M+H)^+$ 508

1-benzyl-N-butyl-2-imino-5-oxo-2,5-dihydro-1H-dipyrido[1,2-a:2',3'-d]pyrimidine-3-carboxamide (8m). Yellow solid; ^{1}H NMR (400 MHz, $CDCl_3$) δ 9.04 (d, *J* = 6.5 Hz, 1H), 7.78 (t, *J* = 6.8 Hz, 1H), 7.52 - 7.49 (m, 1H), 7.38 – 7.29 (m, 7H), 7.14 (t, *J* = 6.0 Hz, 2H), 5.68 (s, 2H), 3.41 (dd, *J* = 12.7, 6.9 Hz, 2H), 1.61 - 1.57 (m, 2H), 1.39 (dd, *J* = 15.2, 7.5 Hz, 2H), 0.93 (t, *J* = 7.3 Hz, 3H); LCMS (electrospray) m/z $(M+H)^+$ 402

1-benzyl-N-(cyclohexylmethyl)-2-imino-5-oxo-2,5-dihydro-1H-dipyrido[1,2-a:2',3'-d]pyrimidine-3-carboxamide (8n). Yellow solid; ^{1}H NMR (400 MHz, $CDCl_3$) δ 9.04 (d, *J* = 6.8 Hz, 1H), 8.96 (s, 1H), 7.82 (t, *J* = 8.0 Hz, 1H), 7.54 (d, *J* = 9.2 Hz, 1H), 7.39 – 7.26 (m, 7H), 7.19 (t, *J* = 7.2 Hz, 1H), 5.75 (s, 2H), 3.26 (t, *J* = 6.4 Hz, 2H), 1.79 – 1.64 (m, 5H), 1.25 – 1.13 (m, 4H), 1.02 – 0.96 (m, 2H); LCMS (electrospray) m/z $(M+H)^+$ 442

N-((1R,2S,5S)-adamantan-2-yl)-1-benzyl-2-imino-5-oxo-2,5-dihydro-1H-dipyrido[1,2-a:2',3'-d]pyrimidine-3-carboxamide (8o). Yellow solid; ^{1}H NMR (400 MHz, DMSO-d_6) δ 11.66 (d, *J* = 8.4 Hz, 1H), 8.97 (d, *J* = 7.2 Hz, 1H), 8.76 (s, 1H), 8.03 – 7.99 (m, 1H), 7.76 (s, 1H), 7.60 (d, *J* = 8.8 Hz, 1H), 7.37 – 7.25 (m, 6H), 5.72 (s, 2H), 4.08 – 4.05 (m, 1H), 1.85 – 1.72 (m, 10H), 1.70 (s, 2H), 1.56 (m, 2H); LCMS (electrospray) m/z $(M+H)^+$ 480

1-benzyl-N-cyclohexyl-2-imino-5-oxo-2,5-dihydro-1H-dipyrido[1,2-a:2',3'-d]pyrimidine-3-carboxamide (8p). Yellow solid; ^{1}H NMR (400 MHz, $CDCl_3$) δ 9.07 (d, *J* = 7.6 Hz, 1H), 8.90 (s, 1H), 7.97

– 7.89 (m, 1H), 7.63 (d, *J* = 9.2 Hz, 1H), 7.40 – 7.26 (m, 8H), 5.87 (s, 2H), 3.91 (brs, 1H), 2.05 – 1.96 (m, 2H), 1.80 – 1.71 (m, 2H), 1.44 – 1.32 (m, 5H), 1.30 – 1.19 (m, 1H); LCMS (electrospray) m/z $(M+H)^+$ 428

1-benzyl-2-imino-5-oxo-2,5-dihydro-1H-dipyrido[1,2-a:2',3'-d]pyrimidine-3-carbonitrile (9a). Yellow solid; ^{1}H NMR (400 MHz, $CDCl_3$) δ 8.95 (d, *J* = 7.1 Hz, 1H), 8.20 (s, 1H), 7.85 – 7.81 (m, 1H), 7.54 (d, *J* = 8.0 Hz, 1H), 7.46 (d, *J* = 7.3 Hz, 2H), 7.31 - 7.28 (m, 2H), 7.24 – 7.21 (m, 1H), 7.14 (t, *J* = 6.4 Hz, 1H), 5.74 (s, 2H); LCMS (electrospray) m/z $(M+H)^+$ 328

1-benzyl-2-imino-3-(phenylsulfonyl)-1H-dipyrido[1,2-a:2',3'-d]pyrimidin-5(2H)-one (9c). Yellow solid; ^{1}H NMR (400 MHz, $CDCl_3$) δ 8.96 (d, *J* = 6.8 Hz, 1H), 8.79 (s, 1H), 8.56 (s, 1H), 7.96 (d, *J* = 7.6 Hz, 2H), 7.79 (ddd, *J* = 8.6, 6.7, 1.6 Hz, 1H), 7.61 (t, *J* = 7.4 Hz, 1H), 7.55 – 7.46 (m, 3H), 7.32 (d, *J* = 7.1 Hz, 2H), 7.23 – 7.17 (m, 3H), 7.10 (d, *J* = 6.8 Hz, 1H), 5.66 (s, 2H); LCMS (electrospray) m/z $(M+H)^+$ 443

(S)-2-imino-5-oxo-1-phenyl-N-(1-phenylethyl)-2,5-dihydro-1H-dipyrido[1,2-a:2',3'-d]pyrimidine-3-carboxamide (10b). Yellow solid; mp = 263°C; ^{1}H NMR (400 MHz, $CDCl_3$) δ 11.42 (s, 1H), 9.13 (s, 1H), 8.99 (d, *J* = 6.8 Hz, 1H), 7.68 – 7.54 (m, 3H), 7.38 (d, *J* = 7.6 Hz, 2H), 7.34 – 7.27 (m, 3H), 7.26 – 7.19 (m, 4H), 7.06 (t, *J* = 6.4 Hz, 1H), 6.67 (s, 1H), 5.33 – 5.28 (m, 1H), 1.54 (d, *J* = 6.8 Hz, 3H); LCMS (electrospray) m/z $(M+H)^+$ 436

(S)-1-(cyclohexylmethyl)-2-imino-5-oxo-N-(1-phenylethyl)-2,5-dihydro-1H-dipyrido[1,2-a:2',3'-d]pyrimidine-3-carboxamide (10c). Yellow solid; mp = 145°C; ^{1}H NMR (400 MHz, $CDCl_3$) δ 8.99 (d, *J* = 6.8 Hz, 1H), 8.91 (s, 1H), 7.90 (brs, 1H), 7.62 (d, *J* = 8.6 Hz, 1H), 7.40 (d, *J* = 7.5 Hz, 2H), 7.33 (t, *J* = 7.5 Hz, 2H), 7.25 – 7.18 (m, 3H), 5.28 – 5.22 (m, 1H), 4.43 (brs, 2H), 1.94 (s, 1H), 1.77 - 1.61 (m, 5H), 1.26 - 1.11 (m, 5H) ; LCMS (electrospray) m/z $(M+H)^+$ 456

(S)-1-benzyl-2-imino-8-methyl-5-oxo-N-(1-phenylethyl)-1,5-dihydro-2H-dipyrido[1,2-a:2',3'-d]pyrimidine-3-carboxamide (11a). Yellow solid; mp = 215°C; ^{1}H NMR (400 MHz, $CDCl_3$); δ 8.90(s, 1H), 8.87(s, 1H), 7.89(d, *J* = 8.0Hz, 1H), 7.64(d, *J* = 8.8Hz, 1H), 7.28-7.34(m, 9H), 7.19-7.23(m, 2H), 5.98(q, *J* = 8.0Hz, 2H), 5.13(q, *J* = 8.8Hz, 1H), 2.50(s, 3H), 1.58(s, 3H); LC/MS (electrospray) m/z $(M+H)^+$464.

(S)-1-benzyl-2-imino-9-methyl-5-oxo-N-(1-phenylethyl)-2,5-dihydro-1H-dipyrido[1,2-a:2',3'-d]pyrimidine-3-carboxamide (11b). Orange solid; mp = 144°C; ^{1}H NMR (400 MHz, $CDCl_3$) δ 8.98 (s, 1H), 8.88 (d, *J* = 7.2 Hz, 1H), 7.36-7.26 (m, 10H), 7.16 (t, *J* = 7.2 Hz, 1H), 7.06 (d, *J* = 6.4 Hz, 1H), 5.95-5.70 (m,

2H), 5.22-5.12 (m, 1H), 2.50 (s, 3H), 1.56 (d, J = 6.4 Hz, 3H);LCMS (electrospray) m/z $(M+H)^+$ 464

(S)-1-benzyl-2-imino-10-methyl-5-oxo-N-(1-phenylethyl)-2,5-dihydro-1H-dipyrido[1,2-a:2',3'-d]pyrimidine-3-carboxamide (11c). Brown solid; ^{1}H NMR (400 MHz, $CDCl_3$) δ 11.18 (br s, 1 H), 8.99 (s, 1H), 8.90 (d, *J* = 6.8 Hz, 1H), 7.64 (d, *J* = 6.8 Hz, 1H), 7.39-7.29 (m, 9 H), 7.21 (t, *J* = 7.2 Hz, 1H), 7.04 (t, *J* = 6.8 Hz, 1H), 5.90-5.50 (m, 2H), 5.28 (quintet, *J* = 7.2 Hz, 1H), 2.44 (s, 3H), 1.52 (d, *J* = 6.8 Hz, 3H); LCMS (electrospray) m/z $(M+H)^+$ 464.

(S)-1-benzyl-2-imino-10-methoxy-5-oxo-N-(1-phenylethyl)-2,5-dihydro-1H-dipyrido[1,2-a:2',3'-d]pyrimidine-3-carboxamide (11d). Yellow solid; ^{1}H NMR (400 MHz, $CDCl_3$) δ 8.98 (s, 1H), 8.66 (d, *J* = 6.7 Hz, 1H), 7.39 – 7.28 (m, 10H), 7.24 – 7.20 (m, 2H), 7.10 – 7.03 (m, 2H), 5.81 - 5.66 (m, 2H), 5.30 – 5.23 (m, 1H), 3.96 (s, 3H), 1.53 (s, 3H); LCMS (electrospray) m/z $(M+H)^+$ 480

(S)-1-benzyl-8-fluoro-2-imino-5-oxo-N-(1-phenylethyl)-2,5-dihydro-1H-dipyrido[1,2-a:2',3'-d]pyrimidine-3-carboxamide (11e). Brown solid; mp = 120°C; ^{1}H NMR (400 MHz, CD_3OD) δ 9.19 (s, 1H), 9.11 (t, *J* = 3.2 Hz, 1H), 8.20-8.15 (m, 1H), 7.83 (dd, *J* = 9.6, 4.8 Hz, 1H), 7.43 (d, *J* = 7.2 Hz, 2H), 7.37-7.24 (m, 8H), 6.03-5.92 (m, 2H), 5.26 (q, *J* = 6.8 Hz, 1H), 1.61 (d, *J* = 7.2 Hz, 3H); LCMS (electrospray) m/z $(M+H)^+$ 468

(S)-1-benzyl-10-fluoro-2-imino-5-oxo-N-(1-phenylethyl)-1,5-dihydro-2H-dipyrido[1,2-a:2',3'-d]pyrimidine-3-carboxamide (Compound 11f). Brown solid; mg = 235°C; ^{1}H NMR (400 MHz, $CDCl_3$); δ 8.87(s, 1H), 8.83(s, 1H), 8.25(d, *J* = 7.2Hz, 1H), 7.87(d, *J* = 8.0Hz, 1H), 7.54(d, *J* = 7.2Hz, 1H), 7.25-7.30(m, 9H), 7.15-7.20(m, 2H), 5.95(q, *J* = 8.0Hz, 2H), 5.11(q, *J* = 7.2Hz, 1H), 1.58(s, 3H); LC/MS (electrospray) m/z $(M+H)^+$ 468.

(S)-1-benzyl-8-chloro-2-imino-5-oxo-N-(1-phenylethyl)-2,5-dihydro-1H-dipyrido[1,2-a:2',3'-d]pyrimidine-3-carboxamide (11h). Yellow solid; mp = 163°C; ^{1}H NMR (400 MHz, $CDCl_3$) δ 9.04 (d, *J* = 1.6 Hz, 1H), 8.98 (br s, 1H), 7.71 (d, *J* = 8.8 Hz, 1H), 7.45 (d, *J* = 9.6 Hz, 1H), 7.38-7.24 (m, 10H), 5.80-5.50 (m, 2H), 5.27 (quintet, *J* = 7.2 Hz, 1H), 1.54 (d, J = 6.8 Hz, 3H); LCMS (electrospray) m/z $(M+H)^+$484, 468 (Cl- isotope pattern).

(S)-1-benzyl-10-chloro-2-imino-5-oxo-N-(1-phenylethyl)-1,5-dihydro-2H-dipyrido[1,2-a:2',3'-d]pyrimidine-3-carboxamide (11i). Brown solid; mp = 237°C; ^{1}H NMR (400 MHz, $CDCl_3$); δ 8.90(s, 1H),

8.87(s, 1H), 8.27(d, *J* = 7.2Hz, 1H), 7.85(d, *J* = 5.2Hz, 1H), 7.34(d, *J* = 7.8Hz, 1H), 7.21-7.33(m, 9H), 7.20-7.22(m, 2H), 6.02(q, *J* = 8.0Hz, 2H), 5.13(q, *J* = 7.2Hz, 1H), 1.55(s, 3H); LC/MS (electrospray) m/z $(M+H)^+$ 484.

(S)-1-benzyl-2-imino-5-oxo-N-(1-phenylethyl)-9-(trifluoromethyl)-2,5-dihydro-1H-dipyrido[1,2-a:2',3'-d]pyrimidine-3-carboxamide (11j). Yellow solid; mp = 165°C; ^{1}H NMR (400 MHz, $CDCl_3$) δ 11.39 (br s, 1H), 9.10 (d, *J* = 7.2 Hz, 1H), 9.03 (br s, 1H), 7.73 (s, 1H), 7.36-7.15 (m, 11H), 5.80-5.49 (m, 2H), 5.27 (quintet, *J* = 6.8 Hz, 1H), 1.54 (d, *J* = 6.4 Hz, 3H); LCMS (electrospray) m/z $(M+H)^+$ 518.

4-(trifluoromethyl)benzyl 1-(1-(3,4-dichlorophenyl)ethyl)-2-imino-8-methyl-5-oxo-1,5-dihydro-2H-dipyrido[1,2-a:2',3'-d]pyrimidine-3-carboxylate (12a). Yellow solid; mp = 119°C; ^{1}H NMR (400 MHz, CD_3OD) δ 8.77 (s, 1H), 8.56 (brs, 1H), 7.85 (d, *J* = 8.4 Hz, 1H), 7.64 (d, *J* = 8.0 Hz, 2H), 7.55 (d, *J* = 10.8 Hz, 3H), 7.47 – 7.40 (m, 2H), 7.31 (d, *J* = 8.0 Hz, 1H), 4.60 (s, 2H), 2.41 (s, 3H), 2.00(d, *J* = 6.8 Hz, 3H),; LCMS (electrospray) m/z $(M+H)^+$ 600, 602 (Cl^- isotope pattern).

1-(4-fluorophenyl)cyclopropyl 2-imino-8-methyl-5-oxo-1-(4-(trifluoromethoxy)benzyl)-1,5-dihydro-2H-dipyrido[1,2-a:2',3'-d]pyrimidine-3-carboxylate (12b). Yellow solid; ^{1}H NMR (400 MHz, CD_3OD); δ 8.91 (br s, 2H), 7.98 (d, *J* = 7.2 Hz, 1H), 7.63 (d, *J* = 9.2 Hz, 1H), 7.46-7.37 (m, 4H), 7.24 (d, *J* = 8.4 Hz, 2H), 7.02 (t, *J* = 8.8 Hz, 2H), 5.74 (br s, 2H), 2.48 (s, 3H), 1.36-1.27 (m, 4H); LCMS (electrospray) m/z $(M+H)^+$ 578.

4-(trifluoromethyl)benzyl 2-imino-8-methyl-5-oxo-1-(4-(trifluoromethoxy)benzyl)-1,5-dihydro-2H-dipyrido[1,2-a:2',3'-d]pyrimidine-3-carboxylate (12c). Yellow solid. ^{1}H NMR (400 MHz, $CDCl_3$); δ 9.13 (s, 1H), 8.81 (s, 1H), 7.73 (d, *J* = 8.8 Hz, 1H), 7.53-7.44 (m, 5H), 7.34 (d, *J* = 8.4 Hz, 2H), 7.15 (d, *J* = 8.0 Hz, 2H), 5.82 (br s, 2H), 4.61 (d, *J* = 5.2 Hz, 2H), 2.43 (s, 3H); LCMS (electrospray) m/z $(M+H)^+$ 602.

[1,1'-biphenyl]-4-ylmethyl 2-imino-8-methyl-5-oxo-1-(4-(trifluoromethoxy)benzyl)-1,5-dihydro-2H-dipyrido[1,2-a:2',3'-d]pyrimidine-3-carboxylate (12d). Yellow solid; ^{1}H NMR (400 MHz, CD_3OD); δ 9.23 (s, 1H), 8.98 (s, 1H), 8.08 (dd, *J* = 9.2, 2.0 Hz, 1H), 7.71 (d, *J* = 9.2 Hz, 1H), 7.63-7.56 (m, 4H), 7.48 (d, *J* = 8.0 Hz, 2H), 7.45-7.40 (m, 4H), 7.35-7.27 (m, 3H), 6.01 (br s, 2H), 4.65 (s, 2H), 2.51 (s, 3H); LCMS (electrospray) m/z $(M+H)^+$ 610.

4.2. Biological evaluation

4.2.1. HCVcc assay

Cell culture derived infectious HCV (HCVcc) was produced by transfection of *in vitro* transcribed HCV RNA genome as described previously [18]. Huh-7.5 cells were seeded in 384-well plates, incubated with serially diluted compounds and inoculated with cell culture adapted HCVcc, expressing an NS5A-GFP fusion protein, 2 h after compound treatment. At 72 h post-infection, HCV infection rates and cytotoxicity were determined as previously reported [19].

4.2.2. HCVpp assay

HCV E1/E2-pseudotyped (or VSV-G pseudotyped as a control) lentiviral particles expressing a *Firefly* luciferase reporter gene were used in HCV pseudoparticle (HCVpp) production by co-transfection of plasmids expressing vesicular stomatitis virus (VSV) envelope and human immunodeficiency virus Gag-Pol as described previously [20]. Comparable amounts of HCVpp and VSVGpp were used in every experiment. Briefly, Huh-7 target cells were plated in 384-well plates, treated with compounds for 2 h followed by transduction with HCVpp or VSVGpp. At 12 h post transduction, the cells were washed with PBS 3-times and cells further incubated in fresh media until 72 h post transduction. Transduction rate and inhibition of HCVpp infection were evaluated by DRC analysis measuring luciferase activity using Bright-Glo (Promega).

4.2.3. HCV replication assay

HCV subgenomic replicon cells expressing an NS5A-GFP fusion protein were seeded in 384-well plates and incubated at 37°C with serially diluted compounds for 3 days [21]. HCV replication was assessed by determining the percentage of GFP-positive cells. The EC_{50} and CC_{50} values were calculated by non-linear regression using Prism 5.0v software (Graph Pad Software) [19].

4.3. Microsomal metabolic stability assay

Compounds (2 μM final concentration in 0.02 % DMSO) were incubated with 0.5 mg/mL human liver (pool of 200, mixed gender, Xenotech) and rat male (BD Gentest) microsomes in potassium phosphate buffer. The

reaction was initiated by the addition of NADPH and stopped either immediately or at 10, 20, 30 and 60 min for a precise estimation of clearance. A triple quadrupole Quattro Premier™ mass spectrometer (Waters, Milford, MA) with electrospray ionization (ESI) was employed for sample analysis. Samples were passed through trapping cartridges (Acquity BEH RP18 50 mm×2.1 mm, 1.7 μm, Waters, Milford, MA) followed by an analytical column. The mobile phases were (A) water with 0.1% of formic acid and (B) acetonitrile with 0.1% of formic acid at a flow rate of 0.4 mL/min. The LC conditions were 5% B at 0min, a linear gradient from 5 to 50% B over 0.5 min, held at 50% for 0.25 min, then ramped from 50 to 95% over 0.25 min, followed by 95% B for 0.75 min and back to 5% B over 0.25 min, then held at 5% B for the remaining 0.75 min. The percentage of the remaining compound was calculated by comparing with the initial quantity at 0 min. Half-life was then calculated based on first-order reaction kinetics.

Acknowledgments

This work was supported by the National Research Foundation of Korea (NRF-No. 2014K1A4A7A01074644) grant funded by the Korean government (MSIP), Gyeonggi-do, and KISTI. We are grateful to Drs. Charles M. Rice (Rockefeller University, New York, USA) and Ralf Bartenschlager (University of Heidelberg, Germany) for kindly providing reagents.

References

[1] Hepatitis C, WHO, (2012).
[2] S. Chevaliez, R. Brillet, E. Lazaro, C. Hezode, J.M. Pawlotsky, Analysis of ribavirin mutagenicity in human hepatitis C virus infection, J Virol, 81 (2007) 7732-7741.
[3] N. Hayashi, T. Takehara, Antiviral therapy for chronic hepatitis C: past, present, and future, J Gastroenterol, 41 (2006) 17-27.
[4] M.P. Manns, H. Wedemeyer, M. Cornberg, Treating viral hepatitis C: efficacy, side effects, and complications, Gut, 55 (2006) 1350-1359.
[5] J. Shepherd, J. Jones, D. Hartwell, P. Davidson, A. Price, N. Waugh, Interferon alpha (pegylated and non-pegylated) and ribavirin for the treatment of mild chronic hepatitis C: a systematic review and economic evaluation, Health Technol Assess, 11 (2007) 1-205, iii.
[6] T. Asselah, N. Boyer, D. Saadoun, M. Martinot-Peignoux, P. Marcellin, Direct-acting antivirals for the treatment of hepatitis C virus infection: optimizing current IFN-free treatment and future perspectives, Liver international : official journal of the International Association for the Study of the Liver, 36 Suppl 1 (2016) 47-57.
[7] E. De Clercq, Current race in the development of DAAs (direct-acting antivirals) against HCV, Biochemical

pharmacology, 89 (2014) 441-452.
[8] B.D. Lindenbach, M.J. Evans, A.J. Syder, B. Wolk, T.L. Tellinghuisen, C.C. Liu, T. Maruyama, R.O. Hynes, D.R. Burton, J.A. McKeating, C.M. Rice, Complete replication of hepatitis C virus in cell culture, Science, 309 (2005) 623-626.
[9] T. Wakita, T. Pietschmann, T. Kato, T. Date, M. Miyamoto, Z. Zhao, K. Murthy, A. Habermann, H.G. Krausslich, M. Mizokami, R. Bartenschlager, T.J. Liang, Production of infectious hepatitis C virus in tissue culture from a cloned viral genome, Nature medicine, 11 (2005) 791-796.
[10] J. Zhong, P. Gastaminza, G. Cheng, S. Kapadia, T. Kato, D.R. Burton, S.F. Wieland, S.L. Uprichard, T. Wakita, F.V. Chisari, Robust hepatitis C virus infection in vitro, Proceedings of the National Academy of Sciences of the United States of America, 102 (2005) 9294-9299.
[11] S. Ciesek, T. von Hahn, C.C. Colpitts, L.M. Schang, M. Friesland, J. Steinmann, M.P. Manns, M. Ott, H. Wedemeyer, P. Meuleman, T. Pietschmann, E. Steinmann, The green tea polyphenol, epigallocatechin-3-gallate, inhibits hepatitis C virus entry, Hepatology, 54 (2011) 1947-1955.
[12] C.O. Bush, M.V. Pokrovskii, R. Saito, P. Morganelli, E. Canales, M.O. Clarke, S.E. Lazerwith, J. Golde, B.G. Reid, K. Babaoglu, N. Pagratis, W. Zhong, W.E.t. Delaney, M.S. Paulson, R.K. Beran, A small-molecule inhibitor of hepatitis C virus infectivity, Antimicrobial agents and chemotherapy, 58 (2014) 386-396.
[13] P.M. Perin, S. Haid, R.J. Brown, J. Doerrbecker, K. Schulze, C. Zeilinger, M. von Schaewen, B. Heller, K. Vercauteren, E. Luxenburger, Y.M. Baktash, F.W. Vondran, S. Speerstra, A. Awadh, F. Mukhtarov, L.M. Schang, A. Kirschning, R. Muller, C.A. Guzman, L. Kaderali, G. Randall, P. Meuleman, A. Ploss, T. Pietschmann, Flunarizine prevents hepatitis C virus membrane fusion in a genotype-dependent manner by targeting the potential fusion peptide within E1, Hepatology, 63 (2016) 49-62.
[14] J.Y. Hwang, M.P. Windisch, S. Jo, K. Kim, S. Kong, H.C. Kim, S. Kim, H. Kim, M.E. Lee, Y. Kim, J. Choi, D.S. Park, E. Park, J. Kwon, J. Nam, S. Ahn, J. Cechetto, J. Kim, M. Liuzzi, Z. No, J. Lee, Discovery and characterization of a novel 7-aminopyrazolo[1,5-a]pyrimidine analog as a potent hepatitis C virus inhibitor, Bioorg. Med. Chem. Lett., 22 (2012) 7297-7301.
[15] K. Yoshida, K. Nakayama, Y. Yokomizo, M. Ohtsuka, M. Takemura, K. Hoshino, H. Kanda, K. Namba, H. Nitanai, J.Z. Zhang, V.J. Lee, W.J. Watkins, MexAB-OprM specific efflux pump inhibitors in Pseudomonas aeruginosa. Part 6: exploration of aromatic substituents, Bioorganic & medicinal chemistry, 14 (2006) 8506-8518.
[16] S. Maiti, S.K. Panja, C. Bandyopadhyay, A one-pot synthesis of the 1-benzopyrano[2,3-b]pyridine moiety from 2-(alkyl/arylamino)-4-oxo-4H-1-benzopyran-3-carbaldehyde, Journal of Hetrocyclic Chemistry, 47 (2010) 973-981.
[17] M. Lee, J. Yang, E. Jo, J.Y. Lee, H.Y. Kim, R. Bartenschlager, E.C. Shin, Y.S. Bae, M.P. Windisch, A Novel Inhibitor IDPP Interferes with Entry and Egress of HCV by Targeting Glycoprotein E1 in a Genotype-Specific Manner, Scientific reports, 7 (2017) 44676.
[18] M. Lee, J. Yang, S. Park, E. Jo, H.Y. Kim, Y.S. Bae, M.P. Windisch, Micrococcin P1, a naturally occurring macrocyclic peptide inhibiting hepatitis C virus entry in a pan-genotypic manner, Antiviral research, 132 (2016) 287-295.
[19] J.Y. Hwang, H.Y. Kim, S. Jo, E. Park, J. Choi, S. Kong, D.S. Park, J.M. Heo, J.S. Lee, Y. Ko, I. Choi, J. Cechetto, J. Kim, J. Lee, Z. No, M.P. Windisch, Synthesis and evaluation of hexahydropyrimidines and diamines as novel hepatitis C virus inhibitors, Eur J Med Chem, 70C (2013) 315-325.
[20] B. Bartosch, J. Dubuisson, F.L. Cosset, Infectious hepatitis C virus pseudo-particles containing functional E1-E2 envelope protein complexes, The Journal of experimental medicine, 197 (2003) 633-642.
[21] V. Lohmann, F. Korner, J. Koch, U. Herian, L. Theilmann, R. Bartenschlager, Replication of subgenomic hepatitis C virus RNAs in a hepatoma cell line, Science, 285 (1999) 110-113.

Highlights:

- An iminodipyridinopyrimidine (IDPP) scaffold was identified by phenotypic HTS using infectious HCV.
- IDPP exhibited anti-HCV activity on early and late steps of the viral cycle, but not on HCV RNA replication.
- One IDPP derivative has a selectivity index >220,000 which is predestinated to conveniently study the HCV life cycle.
- Furthermore, a drugable IDPP lead compound was identified which could be developed to a therapeutic HCV intervention.